JOURNAL OF GUIDANCE, CONTROL, AND DYNAMICS
Vol. 19, No. 5, September–October 1996

New Method for Accurate and Consistent Identification of Modal Parameters

R. M. Lin* and S.-F. Ling†
Nanyang Technological University, Singapore 2263, Singapore

A new method for the estimation of modal parameters is presented. Unlike the majority of existing methods, which involve complicated curvefitting and interpolative procedures, the proposed method calculates the modal parameters by solving the eigenvalue problem of an equivalent eigensystem derived from measured frequency response function (FRF) data. It is developed based on the practical assumption that only one incomplete column of the FRF matrix of the test structure has been measured in a frequency range of interest. All measured FRFs are used simultaneously to construct the equivalent eigensystem matrices from which natural frequencies, damping loss factors, and mode shape vectors of interest are solved. Because the identification problem is reduced to an eigenvalue problem of an equivalent system, natural frequencies and damping loss factors identified are consistent. Further procedures for normalizing the identified eigenvectors so that they become mass normalized are developed. Applications of the method to both numerically simulated and practically measured FRF data are given to demonstrate the practicality of the proposed method, and the results obtained are indeed very promising.

I. Introduction

BECAUSE of the ever increasing demands for quality and reliability of almost all engineering structures, it has become essential nowadays to be able to eliminate or alleviate vibration and its related problems such as fatigue and instability at design stage. Such a design demand requires the development and application of sophisticated modern design methods, which in turn require the availability of detailed and accurate mathematical models. These mathematical models needed should be able to describe adequately the dynamic properties of the structures or components under consideration, and they should, when used, be able to predict structural dynamic response and stress levels and important structural characteristics such as fatigue lives and stability margins. Both a theoretical approach such as finite element analysis and an experimental approach such as modal testing are sought to establish such mathematical models. However, many features of mechanical structures and/or components are difficult to model in theoretical finite element analysis, and the approximations introduced during the structural modeling can lead to wide variations in the predicted dynamic characteristics as shown in a survey paper by Ewins and Imregun.[1] On the other hand, it is accepted nowadays that, because of the advances made in instrumentation and measurement techniques, vibration properties identified from measured data are regarded as closer to the true representation of a structure provided sufficient care is given to experimental and identification procedures. The most appropriate experimental techniques used to construct mathematical models of test structures may be found in the technology of modal testing.

Modal testing can be defined as a process of constructing a mathematical model of the test object by suitable measurements of its vibration characteristics. It has been evolving for more than 40 years, although its full potential has only recently become accessible with the advancement of measurement instrumentation and computer technology. There are many applications where results from a modal test can be used; these include 1) comparison of modal properties, 2) identification of damping and nonlinear effects, 3) structural modification and optimization, and 4) force determination.[2]

During the past few decades, many different methods for modal analysis have been developed to identify structural modal parameters from measured response data. Some of these methods have been found to be quite effective. Comprehensive review of the research on modal identification methods can be found in the work of Ewins[2] and Maia.[3] Depending on the domain where the identification process is carried out, modal analysis techniques can be categorized as time-domain and frequency-domain methods. As one of the frequently used time-domain techniques, the complex exponential method proposed by Brown et al.[4] seeks to calculate the modal parameters by analyzing the impulse response functions that are the inverse Fourier transforms of the measured frequency response function (FRF) data. Based on similar concept, Ibrahim and Mikucik[5,6] developed their time domain method to estimate the modal parameters by curvefitting the measured free decay time response of a system. Numerical aspects in terms of its sensitivity to various parameters of the method were discussed by Pappa and Ibrahim.[7] Following the time series approach in system engineering, identification algorithms[8] have also been developed to estimate modal parameters using measured force and response time signals. More recently, an eigensystem realization algorithm has been developed by Juang and Pappa[9,10] to identify structural modal parameters from measured input-output data and has been found to be very effective. Mathematical correlations of the ERA with other existing methods was discussed by Juang.[11]

There also exist a variety of modal analysis techniques developed in the frequency domain. Depending on the number of modes that a modal analysis algorithm can analyze, methods can be classified as single-degree-of-freedom (SDOF) and multi-degree-of-freedom (MDOF) methods. Pendered and Bishop[12] proposed a simple technique to identify natural frequencies by considering the peaks of measured FRFs and by examining the points where the real part of measured FRFs vanishes. The earliest work on modal analysis was apparently done by Kennedy and Puncu,[13] who demonstrated that the Nyquist plots around resonances are almost circular and thus circles can be fitted to resonance regions of measured FRF data to compute the required natural frequencies and damping ratios. Also based on SDOF assumption, a dynamic stiffness method was developed by Dobson[14] by analyzing FRF data around resonances. On the other hand, there are quite a number of MDOF methods available as reviewed by Maia.[3] In the case where the structure to be identified is lightly damped and so the associated modal constants can be considered as real, an efficient method has been devised by Ewins and Gleeson[15] to estimate modal parameters. A more general approach of using polynomial curvefit to identify modal parameters is discussed by Maia.[3] Furthermore, a polyreference method was developed by Vold and Leuridan[16] to estimate modal parameters by simultaneously analyzing several FRFs. When multi-input

Received July 25, 1995; revision received May 20, 1996; accepted for publication June 6, 1996.

*Lecturer, School of Mechanical and Production Engineering, Nanyang Avenue. Member AIAA.

†Associate Professor, School of Mechanical and Production Engineering, Nanyang Avenue. Member AIAA.

excitations are concerned, identification methods have been developed as discussed by Allemang and Brown.[17] In the case where measured FRF data are from nonlinear structures, some techniques have been developed to detect and to quantify nonlinearity.[18,19]

In the present work, a new analytical method for determining the modal parameters from measured FRF data is developed. The method does not involve any complicated curvefitting and interpolative procedures, but rather it makes full use of the measured FRF data available. It calculates the modal parameters by solving the eigenvalue problem of an equivalent eigensystem derived from measured FRF data, and it is developed based on the practical assumption that only one incomplete column of the FRF matrix of the test structure has been measured in a frequency range of interest. All of the measured FRFs are used simultaneously to construct the equivalent eigensystem matrices from which natural frequencies, damping loss factors, and mode shape vectors of interest are solved. Since the identification problem is reduced to an eigenvalue problem of an equivalent system, natural frequencies and damping loss factors identified are consistent. Further procedures for normalizing the identified eigenvectors so that they become mass normalized are developed. Applications of the method to both numerically simulated and practically measured FRF data are given to demonstrate the practicality of the proposed method, and the results obtained are indeed very promising.

II. Theoretical Development

Suppose that one set of frequency response functions (receptances) $\{\alpha(\omega)\}_i$ at n coordinates of interest has been measured with excitation force being applied at coordinate x_i (x_i can be any coordinate that can be easily accessed physically) and assume that corresponding to the n measured coordinates there exist a mass matrix $[M]$, a stiffness matrix $[K]$, and structural damping matrix $[D]$ that describe the measured receptance data. Then the following fundamental equation can be established:

$$[[K] + j[D] - \omega^2[M]]\{\alpha(\omega)\}_i = \{e\}_i \tag{1}$$

where j is the complex notation defined as $j \equiv \sqrt{-1}$ and $\{e\}_i$ is a vector with its ith element to be unity and all of the others zero. Upon substitution of measured receptance data $\{\alpha(\omega)\}_i$ at measurement frequencies $\omega = \omega_p$ and $\omega = \omega_q$, one has

$$\left[[K] + j[D] - \omega_p^2[M]\right]\{\alpha(\omega_p)\}_i = \{e\}_i \tag{2}$$

$$\left[[K] + j[D] - \omega_q^2[M]\right]\{\alpha(\omega_q)\}_i = \{e\}_i \tag{3}$$

Subtracting Eq. (2) from Eq. (3) and rearranging, one can establish the following relationship:

$$[[K] + j[D]]\{\{\alpha(\omega_q)\}_i - \{\alpha(\omega_p)\}_i\} = [M]\left\{\omega_q^2\{\alpha(\omega_q)\}_i - \omega_p^2\{\alpha(\omega_p)\}_i\right\} \tag{4}$$

When L pair of measurement data points are used, Eq. (4) can be rewritten as

$$[[K] + j[D]][B] = [M][A] \tag{5}$$

where matrices $[A]$ and $[B]$ are

$$[A] = \left[\left\{\omega_{q_1}^2\left\{\alpha\left(\omega_{q_1}\right)\right\}_i - \omega_{p_1}^2\left\{\alpha\left(\omega_{p_1}\right)\right\}_i\right\} \cdots \left\{\omega_{q_L}^2\left\{\alpha\left(\omega_{q_L}\right)\right\}_i - \omega_{p_L}^2\left\{\alpha\left(\omega_{p_L}\right)\right\}_i\right\}\right] \tag{6}$$

$$[B] = \left[\left\{\left\{\alpha\left(\omega_{q_1}\right)\right\}_i - \left\{\alpha\left(\omega_{p_1}\right)\right\}_i\right\} \cdots \left\{\left\{\alpha\left(\omega_{q_L}\right)\right\}_i - \left\{\alpha\left(\omega_{p_L}\right)\right\}_i\right\}\right] \tag{7}$$

and L is assumed to be greater than n ($L \geq n$), which is always possible because measured receptance data points are always plentiful.

Postmultiply Eq. (5) by $[B]^T$, and then Eq. (5) becomes

$$[[K] + j[D]][B][B]^T = [M][A][B]^T \tag{8}$$

Now both matrix $[B][B]^T$ and $[A][B]^T$ are square matrices, and hence an eigenvalue problem of the following form can be defined for the system, which is termed here as a derived system because it is derived purely from the measured receptance data:

$$[[A][B]^T]\{\hat{\phi}\} = \hat{\lambda}[[B][B]^T]\{\hat{\phi}\} \tag{9}$$

which is a generalized complex eigenvalue problem with its generalized mass matrix $[B][B]^T$ to be symmetric and its stiffness matrix $[A][B]^T$ to be nonsymmetric. Such a complex eigenvalue problem can be easily solved by using standard numerical algorithms to obtain all of the eigenvalues $[\cdot\hat{\lambda}.]$ and eigenvectors $[\hat{\phi}]$ of the system. A complex conjugate transpose $[B]^*$ can also be used in Eq. (8) instead of $[B]^T$ to derive the generalized mass and stiffness matrices $[B][B]^*$ and $[A][B]^*$. However, because $[B][B]^*$ is not symmetric, the later formulation necessarily increases memory storage.

However, what are actually required are the eigenvalues $[\cdot\lambda.]$ and eigenvectors $[\phi]$ of the test structure in the measured frequency range that satisfy

$$[[K] + j[D]]\{\phi\} = \lambda[M]\{\phi\} \tag{10}$$

and that cannot be solved directly because system matrices $[M]$ and $[[K] + j[D]]$ are not available. Fortunately, in the measured frequency range of interest, the required eigenvalues $[\cdot\lambda.]$ and eigenvectors $[\phi]$ of the test structure can be computed from their corresponding eigenvalues $[\cdot\hat{\lambda}.]$ and eigenvectors $[\hat{\phi}]$ of the derived system.

Postmultiply both sides of Eq. (8) by $\{\hat{\phi}\}$, and then Eq. (8) becomes

$$[[K] + j[D]][B][B]^T\{\hat{\phi}\} = [M][A][B]^T\{\hat{\phi}\} \tag{11}$$

Upon substitution of Eq. (9) into Eq. (11), Eq. (11) becomes

$$[[K] + j[D]][B][B]^T\{\hat{\phi}\} = \hat{\lambda}[M][B][B]^T\{\hat{\phi}\} \tag{12}$$

By comparing Eq. (12) with Eq. (10), it is not difficult to see that the following relationships exist:

$$[\cdot\lambda.] = [\cdot\hat{\lambda}.] \tag{13}$$

$$[\phi] = [B][B]^T[\hat{\phi}] \tag{14}$$

So simply by solving the eigenvalue problem of the derived system, one can compute eigenvalues and eigenvectors of the test structure in the measurement frequency range corresponding to the n measured coordinates based on Eqs. (13) and (14). However, the thus identified eigenvectors $[\phi]$ are generally not mass normalized, and though they are adequate for most applications in modal analysis, mass normalization becomes necessary for some advanced applications in modal analysis such as finite element model updating, component mode synthesis, etc.

Let the mass-normalized eigenvectors of the test structure be $[\tilde{\phi}]$; then one has

$$[\tilde{\phi}] = [\phi][\cdot\beta.] \tag{15}$$

where $[\cdot\beta.]$ is a complex matrix of scaling factors. Then according to the definition, measured receptances $\{\alpha(\omega)\}_i$ can be written as

$$\{\alpha(\omega)\}_i = \sum_{r=1}^{\infty} \frac{r^{\tilde{\phi}_i}}{\lambda_r - \omega^2}\{\tilde{\phi}\}_r = \sum_{r=1}^{m} \frac{r^{\tilde{\phi}_i}}{\lambda_r - \omega^2}\{\tilde{\phi}\}_r + \sum_{r=m+1}^{\infty} \frac{r^{\tilde{\phi}_i}}{\lambda_r - \omega^2}\{\tilde{\phi}\}_r \tag{16}$$

where λ_r and $\{\tilde{\phi}\}_r$ are the eigenvalue and eigenvector of the rth mode, $r^{\tilde{\phi}_i}$ is the ith element of $\{\tilde{\phi}\}_r$, and m is the number of modes that have been identified in the measured frequency range. Then for

$\omega^2 < Re(\lambda_{m+1})$, the last term on the right-hand side of Eq. (16) can be written as

$$\sum_{r=m+1}^{\infty} \frac{r^{\bar{\phi}_i}}{\lambda_r - \omega^2}\{\bar{\phi}\}_r = \sum_{r=m+1}^{\infty}\left[\sum_{k=0}^{\infty}\left(\frac{\omega^2}{\lambda_r}\right)^k\right]\frac{r^{\bar{\phi}_i}}{\lambda_r}\{\bar{\phi}\}_r \tag{17}$$

The infinite complex series in the brackets is absolutely convergent since $|\omega^2/\lambda_r| < 1$, and by retaining just the first two terms of the series, Eq. (17) becomes

$$\sum_{r=m+1}^{\infty}\left[\sum_{k=0}^{\infty}\left(\frac{\omega^2}{\lambda_r}\right)^k\right]\frac{r^{\bar{\phi}_i}}{\lambda_r}\{\bar{\phi}\}_r$$

$$\cong \sum_{r=m+1}^{\infty}\left[1+\frac{\omega^2}{\lambda_r}\right]\frac{r^{\bar{\phi}_i}}{\lambda_r}\{\bar{\phi}\}_r = \{R_1\} + \omega^2\{R_2\} \tag{18}$$

where $\{R_1\}$ and $\{R_2\}$ are vectors of residue constants. Upon substitution of Eqs. (15) and (18), Eq. (16) becomes

$$\{\alpha(\omega)\}_i = \sum_{r=1}^{m}\frac{\beta_r^2 r^{\phi_i}}{\lambda_r - \omega^2}\{\phi\}_r + \{R_1\} + \omega^2\{R_2\} \tag{19}$$

where β_r $(r = 1, m)$ are unknown scaling factors to be determined. Considering receptance data at three measurement frequencies ω_p, ω_q, and ω_s, the following equations can be established:

$$\{\alpha(\omega_p)\}_i = \sum_{r=1}^{m}\frac{\beta_r^2 r^{\phi_i}}{\lambda_r - \omega_p^2}\{\phi\}_r + \{R_1\} + \omega_p^2\{R_2\} \tag{20a}$$

$$\{\alpha(\omega_q)\}_i = \sum_{r=1}^{m}\frac{\beta_r^2 r^{\phi_i}}{\lambda_r - \omega_q^2}\{\phi\}_r + \{R_1\} + \omega_q^2\{R_2\} \tag{20b}$$

$$\{\alpha(\omega_s)\}_i = \sum_{r=1}^{m}\frac{\beta_r^2 r^{\phi_i}}{\lambda_r - \omega_s^2}\{\phi\}_r + \{R_1\} + \omega_s^2\{R_2\} \tag{20c}$$

By eliminating $\{R_1\}$ and $\{R_2\}$, one has

$$\left(\omega_q^2 - \omega_p^2\right)\{\alpha(\omega_s)\}_i + \left(\omega_p^2 - \omega_s^2\right)\{\alpha(\omega_q)\}_i + \left(\omega_s^2 - \omega_q^2\right)\{\alpha(\omega_p)\}_i$$

$$= \left(\omega_q^2 - \omega_p^2\right)\sum_{r=1}^{m}\frac{\beta_r^2 r^{\phi_i}}{\lambda_r - \omega_s^2}\{\phi\}_r + \left(\omega_p^2 - \omega_s^2\right)\sum_{r=1}^{m}\frac{\beta_r^2 r^{\phi_i}}{\lambda_r - \omega_q^2}\{\phi\}_r$$

$$+ \left(\omega_s^2 - \omega_q^2\right)\sum_{r=1}^{m}\frac{\beta_r^2 r^{\phi_i}}{\lambda_r - \omega_p^2}\{\phi\}_r \equiv [E_{pqs}]\{\sigma\} = \{\delta_{pqs}\} \tag{21}$$

where $[E_{pqs}]$, $\{\sigma\}$, and $\{\delta_{pqs}\}$ are

$$[E_{pqs}] = [(\gamma_{1s} + \gamma_{1q} + \gamma_{1p})\{\phi\}_1 \quad (\gamma_{2s} + \gamma_{2q} + \gamma_{2p})\{\phi\}_2$$

$$\cdots \quad (\gamma_{ms} + \gamma_{mq} + \gamma_{mp})\{\phi\}_m]$$

$$\{\delta_{pqs}\} = \left(\omega_q^2 - \omega_p^2\right)\{\alpha(\omega_s)\}_i + \left(\omega_p^2 - \omega_s^2\right)\{\alpha(\omega_q)\}_i \tag{22}$$

$$+ \left(\omega_s^2 - \omega_q^2\right)\{\alpha(\omega_p)\}_i$$

$$\{\sigma\} = \left\{\beta_1^2, \beta_2^2, \ldots, \beta_m^2\right\}^T, \qquad \gamma_{rs} = \left(\omega_q^2 - \omega_p^2\right)\frac{r^{\phi_i}}{\lambda_r - \omega_s^2}$$

$$\gamma_{rq} = \left(\omega_p^2 - \omega_s^2\right)\frac{r^{\phi_i}}{\lambda_r - \omega_q^2}, \qquad \gamma_{rp} = \left(\omega_s^2 - \omega_q^2\right)\frac{r^{\phi_i}}{\lambda_r - \omega_p^2}$$

When L' sets of measured data points are used, Eq. (21) becomes a set of overdetermined linear algebraic equations as

$$\begin{bmatrix}\left[E_{pqs}^{(1)}\right]\\ \left[E_{pqs}^{(2)}\right]\\ \vdots\\ \left[E_{pqs}^{(L')}\right]\end{bmatrix}\{\sigma\} = \begin{Bmatrix}\left\{\delta_{pqs}^{(1)}\right\}\\ \left\{\delta_{pqs}^{(2)}\right\}\\ \vdots\\ \left\{\delta_{pqs}^{(L')}\right\}\end{Bmatrix} \tag{23}$$

which can be solved as[20]

$$\{\sigma\} = \left[\sum_{r=1}^{L'}\left[E_{pqs}^{(r)}\right]^T\left[E_{pqs}^{(r)}\right]\right]^{-1}\left\{\sum_{r=1}^{L'}\left[E_{pqs}^{(r)}\right]^T\left[\delta_{pqs}^{(r)}\right]\right\} \tag{24}$$

With $\{\sigma\}$ being computed, the required mass-normalized eigenvectors of the test structure in the measured frequency range can be easily obtained as

$$\{\bar{\phi}\}_r = \beta_r\{\phi\}_r = \sqrt{\sigma_r}\{\phi\}_r \qquad (r = 1, m) \tag{25}$$

In the case when a structure to be identified possesses rigid-body mode(s), the identification procedure for the derivation of eigenvalues and unscaled eigenvectors is the same. In the process of mass normalization, however, the response contribution as a result of the rigid-body mode(s) should be added into Eq. (19), and Eq. (19) thus becomes

$$\{\alpha(\omega)\}_i = \frac{1}{\omega^2}\{R_0\} + \sum_{r=1}^{m}\frac{\beta_r^2 r^{\phi_i}}{\lambda_r - \omega^2}\{\phi\}_r + \{R_1\} + \omega^2\{R_2\} \tag{26}$$

Following a similar procedure, the unknown scaling factors $\{\sigma\}$ can be solved based on Eq. (26) by employing receptance data at different measurement frequencies. However, since in this case there are three unknown vectors that need to be eliminated, receptance data at four measurement frequencies are needed each time to establish the linear algebraic equations required.

The identification and normalization procedures proposed are also applicable to structures with repeated modes. Suppose that modes Γ and $\Gamma + 1$ are repeated; then from Eq. (16), measured receptances $\{\alpha(\omega)\}_i$ can be written as

$$\{\alpha(\omega)\}_i = \sum_{r=1}^{\Gamma-1}\frac{r^{\bar{\phi}_i}}{\lambda_r - \omega^2}\{\bar{\phi}\}_r + \sum_{r=\Gamma+2}^{\infty}\frac{r^{\bar{\phi}_i}}{\lambda_r - \omega^2}\{\bar{\phi}\}_r$$

$$+ \frac{1}{\lambda_\Gamma - \omega^2}\left\{\Gamma^{\bar{\phi}_i}\{\bar{\phi}\}_\Gamma + (\Gamma+1)^{\bar{\phi}_i}\{\bar{\phi}\}_{\Gamma+1}\right\} \tag{27}$$

When the proposed method is applied, eigenvalues and eigenvectors of nonrepeated modes in the frequency range of interest will be correctly identified. The two repeated modes will be identified as one single mode with its eigenvalue being computed correctly as λ_Γ and eigenvector as $\{\Gamma^{\bar{\phi}_i}\{\bar{\phi}\}_\Gamma + (\Gamma+1)^{\bar{\phi}_i}\{\bar{\phi}\}_{\Gamma+1}\}$, which is a linear combination of $\{\bar{\phi}\}_\Gamma$ and $\{\bar{\phi}\}_{\Gamma+1}$.

III. Relationship Between Identified and Exact Eigenvalues and Eigenvectors

From the preceding theoretical development, it is assumed that the identified eigenvalues and eigenvectors are those of the reduced model whose number of DOF is the same as that of measured coordinates. However, what need to be identified are those eigenvalues and eigenvectors of the actual test structure whose number of DOF is, in theory, infinite. Therefore, it is necessary to establish what are the relationships between identified and exact eigenvalues and eigenvectors, what are the assumptions involved in the theoretical development of the method, and how these assumptions affect the accuracy of identified modal properties.

It is to be proved here that once it is assumed that the measured receptance $\{\alpha(\omega)\}_i$ can be written as

$$\{\alpha(\omega)\}_i = \sum_{r=1}^{n}\frac{r^{\bar{\phi}_i}}{\bar{\lambda}_r - \omega^2}\{\bar{\phi}\}_r \tag{28}$$

where n is the number of measured coordinates and $\bar{\lambda}_r$ and $\{\bar{\phi}\}_r$ are the rth exact eigenvalues and mass-normalized eigenvector of the test structure, the identified modal parameters from the proposed method are exact. Since under this assumption the matrices $[A]$ and $[B]$ become

$$[A] = \left[\sum_{r=1}^{n}\left(\frac{\omega_{q_1}^2 r^{\bar{\phi}_i}}{\bar{\lambda}_r - \omega_{q_1}^2} - \frac{\omega_{p_1}^2 r^{\bar{\phi}_i}}{\bar{\lambda}_r - \omega_{p_1}^2}\right)\{\bar{\phi}\}_r\right.$$

$$\left.\cdots \quad \sum_{r=1}^{n}\left(\frac{\omega_{q_L}^2 r^{\bar{\phi}_i}}{\bar{\lambda}_r - \omega_{q_L}^2} - \frac{\omega_{p_L}^2 r^{\bar{\phi}_i}}{\bar{\lambda}_r - \omega_{p_L}^2}\right)\{\bar{\phi}\}_r\right] \tag{29}$$

$$[B] = \left[\sum_{r=1}^{n} \left(\frac{r^{\bar{\phi}_i}}{\bar{\lambda}_r - \omega_{q_1}^2} - \frac{r^{\bar{\phi}_i}}{\bar{\lambda}_r - \omega_{p_1}^2} \right) \{\bar{\phi}\}_r \right.$$

$$\left. \cdots \sum_{r=1}^{n} \left(\frac{r^{\bar{\phi}_i}}{\bar{\lambda}_r - \omega_{q_L}^2} - \frac{r^{\bar{\phi}_i}}{\bar{\lambda}_r - \omega_{p_L}^2} \right) \{\bar{\phi}\}_r \right] \tag{30}$$

and so matrices $[A][B]^T$ and $[B][B]^T$ become

$$[A][B]^T = \sum_{r=1}^{n} \sum_{s=1}^{n} \sum_{k=1}^{L} \left(\frac{\omega_{q_k}^2 r^{\bar{\phi}_i}}{\bar{\lambda}_r - \omega_{q_k}^2} - \frac{\omega_{p_k}^2 r^{\bar{\phi}_i}}{\bar{\lambda}_r - \omega_{p_k}^2} \right)$$

$$\times \left(\frac{s^{\bar{\phi}_i}}{\bar{\lambda}_s - \omega_{q_k}^2} - \frac{s^{\bar{\phi}_i}}{\bar{\lambda}_s - \omega_{p_k}^2} \right) \left[\{\bar{\phi}\}_r \{\bar{\phi}\}_s^T \right]$$

$$= \sum_{r=1}^{n} \sum_{s=1}^{n} \sum_{k=1}^{L} \bar{\lambda}_r \left(\frac{r^{\bar{\phi}_i}}{\bar{\lambda}_r - \omega_{q_k}^2} - \frac{r^{\bar{\phi}_i}}{\bar{\lambda}_r - \omega_{p_k}^2} \right)$$

$$\times \left(\frac{s^{\bar{\phi}_i}}{\bar{\lambda}_s - \omega_{q_k}^2} - \frac{s^{\bar{\phi}_i}}{\bar{\lambda}_s - \omega_{p_k}^2} \right) \left[\{\bar{\phi}\}_r \{\bar{\phi}\}_s^T \right] \tag{31}$$

$$[B][B]^T = \sum_{r=1}^{n} \sum_{s=1}^{n} \sum_{k=1}^{L} \left(\frac{r^{\bar{\phi}_i}}{\bar{\lambda}_r - \omega_{q_k}^2} - \frac{r^{\bar{\phi}_i}}{\bar{\lambda}_r - \omega_{p_k}^2} \right)$$

$$\times \left(\frac{s^{\bar{\phi}_i}}{\bar{\lambda}_s - \omega_{q_k}^2} - \frac{s^{\bar{\phi}_i}}{\bar{\lambda}_s - \omega_{p_k}^2} \right) \left[\{\bar{\phi}\}_r \{\bar{\phi}\}_s^T \right] \tag{32}$$

where the following identity equation has been used in the derivation of Eq. (31):

$$\frac{\omega_{q_k}^2 r^{\bar{\phi}_i}}{\bar{\lambda}_r - \omega_{q_k}^2} - \frac{\omega_{p_k}^2 r^{\bar{\phi}_i}}{\bar{\lambda}_r - \omega_{p_k}^2} = \bar{\lambda}_r \left(\frac{r^{\bar{\phi}_i}}{\bar{\lambda}_r - \omega_{q_k}^2} - \frac{r^{\bar{\phi}_i}}{\bar{\lambda}_r - \omega_{p_k}^2} \right) \tag{33}$$

Let v_{rs} be defined as

$$v_{rs} = \sum_{k=1}^{L} \left(\frac{r^{\bar{\phi}_i}}{\bar{\lambda}_r - \omega_{q_k}^2} - \frac{r^{\bar{\phi}_i}}{\bar{\lambda}_r - \omega_{p_k}^2} \right) \left(\frac{s^{\bar{\phi}_i}}{\bar{\lambda}_s - \omega_{q_k}^2} - \frac{s^{\bar{\phi}_i}}{\bar{\lambda}_s - \omega_{p_k}^2} \right) \tag{34}$$

Then Eqs. (31) and (32) can be written as

$$[A][B]^T = \sum_{r=1}^{n} \sum_{s=1}^{n} \bar{\lambda}_r v_{rs} \{\bar{\phi}\}_r \{\bar{\phi}\}_s^T = [\bar{\phi}][\cdot\bar{\lambda}.][v][\bar{\phi}]^T \tag{35}$$

$$[B][B]^T = \sum_{r=1}^{n} \sum_{s=1}^{n} v_{rs} \{\bar{\phi}\}_r \{\bar{\phi}\}_s^T = [\bar{\phi}][v][\bar{\phi}]^T \tag{36}$$

Then the eigenvalue problem $[A][B]^T\{\hat{\phi}\} = \hat{\lambda}[B][B]^T\{\hat{\phi}\}$ becomes

$$[\bar{\phi}][\cdot\bar{\lambda}.][v][\bar{\phi}]^T\{\hat{\phi}\} = \hat{\lambda}[\bar{\phi}][v][\bar{\phi}]^T\{\hat{\phi}\} \tag{37}$$

Let $\{\delta\} = [v][\bar{\phi}]^T\{\hat{\phi}\}$ and premultiply both sides of Eq. (37) by $[\bar{\phi}]^{-1}$, and then one has

$$[\cdot\bar{\lambda}.]\{\delta\} = \hat{\lambda}\{\delta\} \tag{38}$$

The eigenvalues and eigenvectors of Eq. (38) are

$$\hat{\lambda}_r = \bar{\lambda}_r, \qquad \{\delta\}_r = \{e\}_r \qquad \text{for} \qquad r = 1, 2, \ldots, n \tag{39}$$

From the definition of $\{\delta\}$, one has

$$\{e\}_r = [v][\bar{\phi}]^T\{\hat{\phi}\}_r \tag{40}$$

Premultiply both sides of Eq. (40) by $[\bar{\phi}]$, and then Eq. (40) becomes

$$\{\bar{\phi}\}_r = [\bar{\phi}][v][\bar{\phi}]^T\{\hat{\phi}\}_r = [B][B]^T\{\hat{\phi}\}_r \tag{41}$$

Thus, the identified eigenvalues are exactly the same as those of the test structure and the identified eigenvectors are related to the exact eigenvectors of the test structure by a known matrix transformation.

To examine how the assumption of Eq. (28) will affect the identification accuracy, it is necessary to investigate how close is the receptance of Eq. (28) to its true counterpart, which is expressed as

$$\{\alpha(\omega)\}_i = \sum_{r=1}^{\infty} \frac{r^{\bar{\phi}_i}}{\bar{\lambda}_r - \omega^2} \{\bar{\phi}\}_r \tag{42}$$

Because of the quadratic separation terms on the numerator, experience has shown that for lower m modes of interest, if the number of measured coordinates n is much larger than m ($n \geq 2m$, a condition that is satisfied in most practical cases), then the approximation of Eq. (28) becomes, indeed, very true and the identified modal parameters become very accurate. This will be demonstrated later in numerical case examples.

IV. Separation of Physical and Computational Modes

Since the number of modes m to be identified in the measured frequency range is in general much less than the number of measured coordinates n while the eigensolution identifies n modes each time, some of the remaining $n-m$ modes are computational whose existence is purely a result of the numerical process involved, and others represent the modes of the test structure that are beyond the measurement frequency range and whose identification itself constitutes an important research area. This section develops a procedure that will be used to separate the m genuine physical modes from the n computed modes. Such a procedure is developed based on the assumption that for the genuine physical modes they should consistently appear no matter what combination of measurement data points are used, whereas for computational modes, they are very sensitive to the choice of data points. So, by choosing a different number of data sets L and different combinations of data separation $\Delta n_k = q_k - p_k$ and then comparing their eigenproperties, one can identify a specific mode whether it is a structural property or a computational DOF.

For data combination of $L = L_1$ and $\Delta n_k = \Delta n_k^{(1)} = q_k^{(1)} - p_k^{(1)}$ ($k = 1, 2, \ldots, L_1$), one has

$$\left[[A_1][B_1]^T\right]\left\{\hat{\phi}^{(1)}\right\} = \hat{\lambda}^{(1)}\left[[B_1][B_1]^T\right]\left\{\hat{\phi}^{(1)}\right\} \tag{43}$$

For data combination of $L = L_2$ and $\Delta n_k = \Delta n_k^{(2)} = q_k^{(2)} - p_k^{(2)}$ ($k = 1, 2, \ldots, L_2$), one has

$$\left[[A_2][B_2]^T\right]\left\{\hat{\phi}^{(2)}\right\} = \hat{\lambda}^{(2)}\left[[B_2][B_2]^T\right]\left\{\hat{\phi}^{(2)}\right\} \tag{44}$$

By solving eigenvalue problems of Eqs. (43) and (44), eliminating those modes whose eigenvalues have negative real parts, negative imaginary parts, or the associated frequencies that are beyond the measurement frequency range, and sorting the remaining modes in ascending order according to the magnitudes of the real parts of the eigenvalues, one has the following:

$$\left\{\hat{\lambda}^{(1)}\right\}^T = \left\{\hat{\lambda}_1^{(1)}, \hat{\lambda}_2^{(1)}, \ldots, \hat{\lambda}_r^{(1)}\right\}^T$$

$$\left[\hat{\phi}^{(1)}\right] = \left[\left\{\hat{\phi}^{(1)}\right\}_1 \quad \left\{\hat{\phi}^{(1)}\right\}_2 \quad \cdots \quad \left\{\hat{\phi}^{(1)}\right\}_r\right] \tag{45}$$

$$\left\{\hat{\lambda}^{(2)}\right\}^T = \left\{\hat{\lambda}_1^{(2)}, \hat{\lambda}_2^{(2)}, \ldots, \hat{\lambda}_v^{(2)}\right\}^T$$

$$\left[\hat{\phi}^{(2)}\right] = \left[\left\{\hat{\phi}^{(2)}\right\}_1 \quad \left\{\hat{\phi}^{(2)}\right\}_2 \quad \cdots \quad \left\{\hat{\phi}^{(2)}\right\}_v\right] \tag{46}$$

Let the error bounds for eigenvalues be ε_λ and eigenvectors be ε_ϕ (the actual values of ε_λ and ε_ϕ depend on measurement accuracy and generally values between 1–2% are recommended); then the following procedure can be used to judge whether the ith mode

$(\hat{\lambda}_i^{(1)}, \{\hat{\phi}^{(1)}\}_i)$ is one of the genuine modes of the test structure. First define a vector $\{\chi\}_i$ as

$$\{\chi\}_i^T \equiv \frac{\left\{Re\left(\hat{\lambda}^{(2)}\right)\right\}^T}{Re\left(\hat{\lambda}_i^{(1)}\right)} = \left\{\frac{Re\left(\hat{\lambda}_1^{(2)}\right)}{Re\left(\hat{\lambda}_i^{(1)}\right)}, \frac{Re\left(\hat{\lambda}_2^{(2)}\right)}{Re\left[\hat{\lambda}_i^{(1)}\right]}, \ldots, \frac{Re\left(\hat{\lambda}_v^{(2)}\right)}{Re\left(\hat{\lambda}_i^{(1)}\right)}\right\}^T \quad (47)$$

Determine the number v of modes that satisfy

$$1 - \varepsilon_\lambda \le \chi_j \le 1 + \varepsilon_\lambda \Rightarrow j = n_i, n_i + 1, \ldots, n_i + v - 1 \quad (48)$$

If there is no such χ_j that satisfies Eq. (48), i.e., $v = 0$, then the ith mode $(\hat{\lambda}_i^{(1)}, \{\hat{\phi}^{(1)}\}_i)$ is one of the computational modes. If $v \neq 0$, then compute the following confidence vector $\{c\}_i$ as

$$c_k = \frac{\left\{\hat{\phi}^{(2)}\right\}_{n_i+k}^T \left\{\hat{\phi}^{(1)}\right\}_i}{\sqrt{\left\{\hat{\phi}^{(2)}\right\}_{n_i+k}^T \left\{\hat{\phi}^{(2)}\right\}_{n_i+k}} \sqrt{\left\{\hat{\phi}^{(1)}\right\}_i^T \left\{\hat{\phi}^{(1)}\right\}_i}} \qquad k = 0, 1, \ldots, v-1 \quad (49)$$

If $\{\hat{\phi}^{(1)}\}_i$ is a genuine mode and it corresponds to $\{\hat{\phi}^{(2)}\}_{n_i+k}$, then $c_k = 1$ and all of the other elements of $\{c\}_i$ will be much less than 1. Based on this observation, perform the following comparison:

$$(1 - \varepsilon_\phi) \le Re(c_k) \le (1 + \varepsilon_\phi) \quad (50)$$

If there is no such $c_k (k = 0, 2, \ldots, v-1)$ that satisfies Eq. (50), then the ith mode $(\hat{\lambda}_i^{(1)}, \{\hat{\phi}^{(1)}\}_i)$ is not genuine but computational. If there is only one c_k that satisfies Eq. (50), then the ith mode is a genuine mode. If there is more than one c_k that satisfies Eq. (50), then one more eigensolution with $L = L_3$ and $\Delta n_k = \Delta n_k^{(3)} = q_k^{(3)} - p_k^{(3)} (k = 1, 2, \ldots, L_3)$ needs to be performed and the preceding separation procedure repeated. However, such a situation is rarely encountered in practice. To summarize, the complete identification procedures are as follows.

1) Construct matrices $[A]$ and $[B]$ according to Eqs. (7) and (8).

2) Perform an eigensolution of $[A][B]^T\{\hat{\phi}\} = \hat{\lambda}[B][B]^T\{\hat{\phi}\}$ to obtain $[\hat{\cdot\lambda}.]$, and $[\hat{\phi}]$.

3) Separate physical modes from computational modes based on Eqs. (48) and (50).

4) Compute eigenvalues and unscaled eigenvectors $[\cdot\lambda.] = [\hat{\cdot\lambda}.]$ and $[\phi] = [B][B]^T[\hat{\phi}]$.

5) Find the scaling factors $[\cdot\beta.]$ to mass normalize $[\tilde{\phi}] = [\phi][\cdot\beta.]$.

V. Applications of the Proposed Method

Theoretical aspects of the proposed method have been discussed and now its practical applicability needs to be assessed. Based on theoretical development, a computer software has been devised that takes the measured FRFs as input data and outputs the identified natural frequencies, damping loss factors, and mass-normalized mode shape vectors in the frequency range of interest. A complex QZ algorithm proposed by Moler and Steward[21] was used to solve the generalized complex eigenvalue problem involved. Numerically simulated FRF data of a beam and damped sandwich plate structures as well as practically measured FRFs of a beam test rig were used to validate the proposed method.

Application to Simulated FRF Data

The first example problem is a fixed-fixed beam whose physical geometry and material properties are shown in Fig. 1. The beam was modeled using finite elements by discretizing it into 30 identical beam elements. The mass matrix $[M]$ and stiffness matrix $[K]$, which are of dimension 58 × 58, were then established. The damping in this case is assumed to be proportional as $[D] = 0.01[K]$. With these mass, stiffness, and damping matrices, receptances of the beam structure can be computed, and it is assumed that only six coordinates ($x_2, x_7, x_{12}, x_{17}, x_{22}$, and x_{27}) were measured with excitation being applied at coordinate x_2. One typical simulated experimental receptance $\alpha_{22}(\omega)$ is shown in Fig. 2 together with its regenerated (using identified modal parameters) counterpart. It was assumed that 300 frequency lines have been measured in a frequency range from 10–300 Hz in which four modes were included. By taking all of the six simulated experimental receptances simultaneously to construct the derived system matrices $[B][B]^T$ and $[A][B]^T$ and then solving the complex eigenvalue problem of the derived system, the first four natural frequencies, damping loss factors, and mass-normalized mode shapes corresponding to the six measured coordinates were calculated. The identified natural frequencies and damping loss factors with receptance data being contaminated by different levels of simulated measurement noise are shown in Table 1 in which 100 frequency data pairs ($L = 100$) were used with frequency separation of $\Delta n_k = q_k - p_k = 15$ in the construction of $[A]$ and $[B]$ matrices. Simulated random measurement noise was added to the receptance data so that the perturbed receptance becomes $\alpha(\omega) = \alpha(\omega) \times (1 + \xi\gamma(\omega)/100)$ for the case of $\xi\%$ noise, where $\gamma(\omega)$ is a random variable that satisfies $-1 \le \gamma(\omega) \le 1$. As can be seen from Table 1, the identified results are very accurate as compared with their exact values even in the case of a high level of noise contamination. The identified eigenvector elements are also very accurate as one can see from the regenerated receptance curve of Fig. 2, which is indeed very close to the simulated experimental receptance curve for the

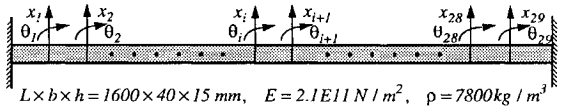

Fig. 1 Beam structure used in numerical case studies.

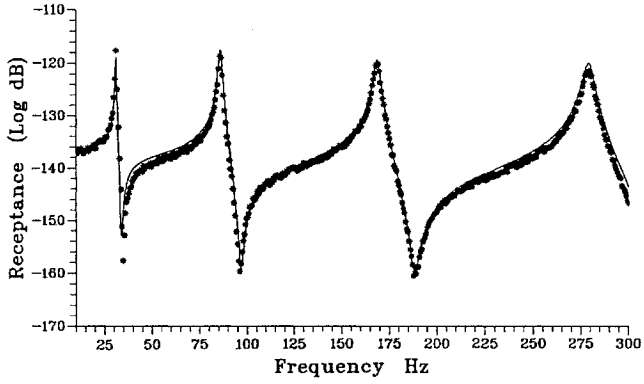

Fig. 2 Simulated and regenerated receptances of beam structure: * * *, simulated and ——, regenerated.

Table 1 Identified natural frequencies and loss factors (beam structure)

Mode no.	Exact ω_r/η_r	Identified ω_r/η_r 0% noise	5% noise	% error	10% noise	% error	20% noise	% error
ω_1	31.2516	31.2516	31.2438	−0.02496	31.2406	−0.03520	31.2215	−0.09632
ω_2	86.1466	86.1466	86.1494	0.00325	86.1519	0.00615	86.2269	0.09321
ω_3	168.883	168.883	168.882	−0.00059	168.880	−0.00178	169.057	0.10303
ω_4	279.179	279.179	279.157	−0.00788	279.130	−0.01755	278.952	−0.08131
η_1	0.01000	0.01000	0.01003	0.30000	0.01022	2.20000	0.01041	4.10000
η_2	0.01000	0.01000	0.01007	0.70000	0.01027	2.70000	0.01033	3.30000
η_3	0.01000	0.01000	0.01002	0.20000	0.00991	−0.90000	0.01012	1.20000
η_4	0.01000	0.01000	0.00996	−0.40000	0.01013	1.30000	0.00983	−1.70000

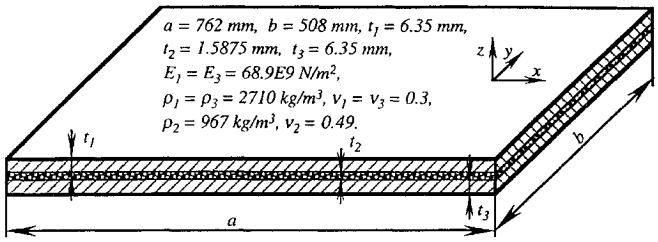

Fig. 3 Sandwich plate structure.

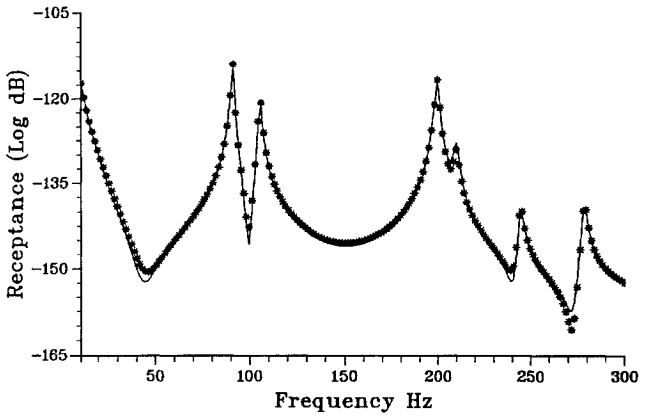

Fig. 4 Simulated and regenerated receptances of sandwich plate structure: * * *, simulated and ——, regenerated.

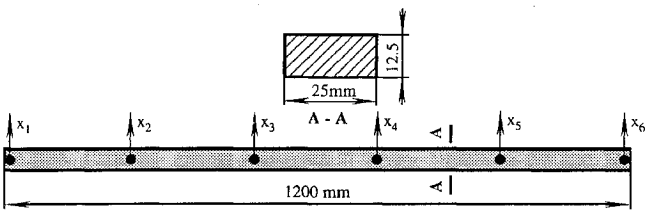

Fig. 5 Aluminum beam test rig.

case when 20% measurement noise was considered. To quantify the accuracy of identified eigenvectors, define the following:

$$\kappa_r = \frac{\|\{\tilde{\phi}\}_r - \{\bar{\phi}\}_r\|}{\|\{\bar{\phi}\}_r\|} \tag{51}$$

where $\{\tilde{\phi}\}_r$ and $\{\bar{\phi}\}_r$ are the identified and the exact mass-normalized eigenvectors. In the case of 20% noise, the κ_r values for the four modes identified are $\kappa_1 = 3.03\%$, $\kappa_2 = 2.71\%$, $\kappa_3 = 5.14\%$, and $\kappa_4 = 6.05\%$.

Also, a sandwich plate with a constrained damping layer as shown in Fig. 3 was considered. As compared with the beam structure, the plate is assumed to be tested under free-free support conditions, and the damping, which comes from the viscoelastic core, is no longer proportional. In the finite element modeling, eight-node brick elements were used both for the two constraining layers and the viscoelastic core. Each layer was modeled by 64 brick elements, and so the total number of DOF of the model is $N = 81 \times 3 \times 4 = 972$ for considering three DOFs at each node with 81 nodes at each layer of nodes for four layers. The constraining layers are aluminum plates, and the viscoelastic core is ISD-112 (3-M Corporation). With this finite element model, plate receptances were then computed, and it was assumed that only 25 evenly distributed coordinates in the z direction on the top surface of the sandwich plate were measured. One typical simulated experimental receptance with 10% random noise is shown in Fig. 4 together with its regenerated counterpart. The identified natural frequencies and damping loss factors with receptance data being contaminated by different levels of simulated measurement noise are shown in Table 2. Again, the identified results are very accurate as can be seen from Table 2 and the regenerated receptance curve of Fig. 4.

Application to Real Measured FRF Data

The method has so far been rigorously assessed by using numerically simulated FRF data, and it is further applied here to the case of real measured FRF data. An aluminum beam test rig as shown in Fig. 5 was tested under free-free support conditions by using step sine testing based on frequency response analyzer. The whole measurement setup is shown in Fig. 6, and the acquisition of FRF

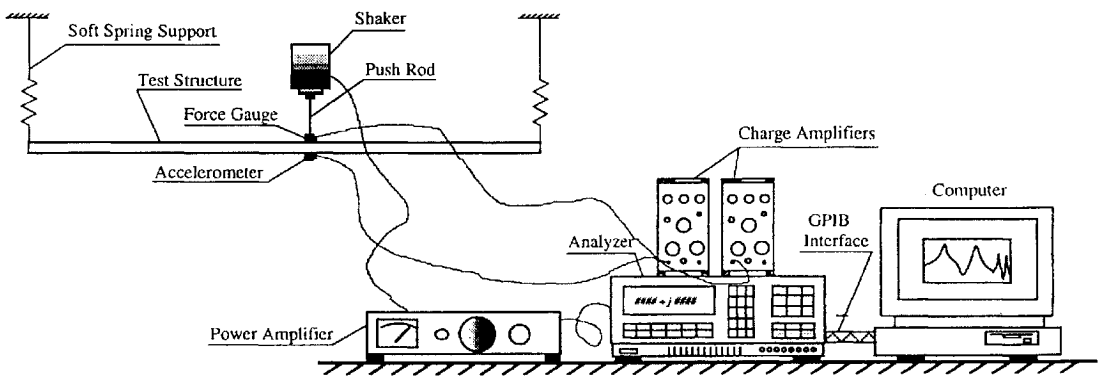

Fig. 6 Illustration of measurement setup.

Table 2 Identified natural frequencies and loss factors (sandwich plate)

Mode no.	Exact ω_r/η_r	Identified ω_r/η_r 0% noise	% error	5% noise	% error	10% noise	% error
ω_1	90.06839	90.06839	0.00000	90.06888	5.53E−4	90.07439	0.00666
ω_2	104.6208	104.6208	0.00000	104.5986	−0.02122	104.5429	−0.07446
ω_3	198.7381	198.7381	0.00000	198.7113	−0.01499	198.7011	−0.01912
ω_4	209.2669	209.2669	0.00000	209.4014	0.04995	210.8953	0.77815
ω_5	243.8936	243.8936	0.00000	244.0530	0.06536	244.5842	0.28316
ω_6	278.0118	278.0101	−6.12E−4	277.8316	−0.06482	278.6702	0.23682
η_1	0.015359	0.015359	0.00000	0.015140	−1.42587	0.014892	−3.04056
η_2	0.017608	0.017608	0.00000	0.017591	−0.09655	0.017309	−1.69809
η_3	0.010837	0.010837	0.00000	0.010992	1.43028	0.011095	2.38073
η_4	0.014703	0.014706	2.04E−2	0.013867	−5.70515	0.013021	−11.4398
η_5	0.011275	0.011273	−1.77E−2	0.011560	2.54590	0.012305	9.13525
η_6	0.009607	0.009607	0.00000	0.009121	−5.05881	0.008471	−11.8247

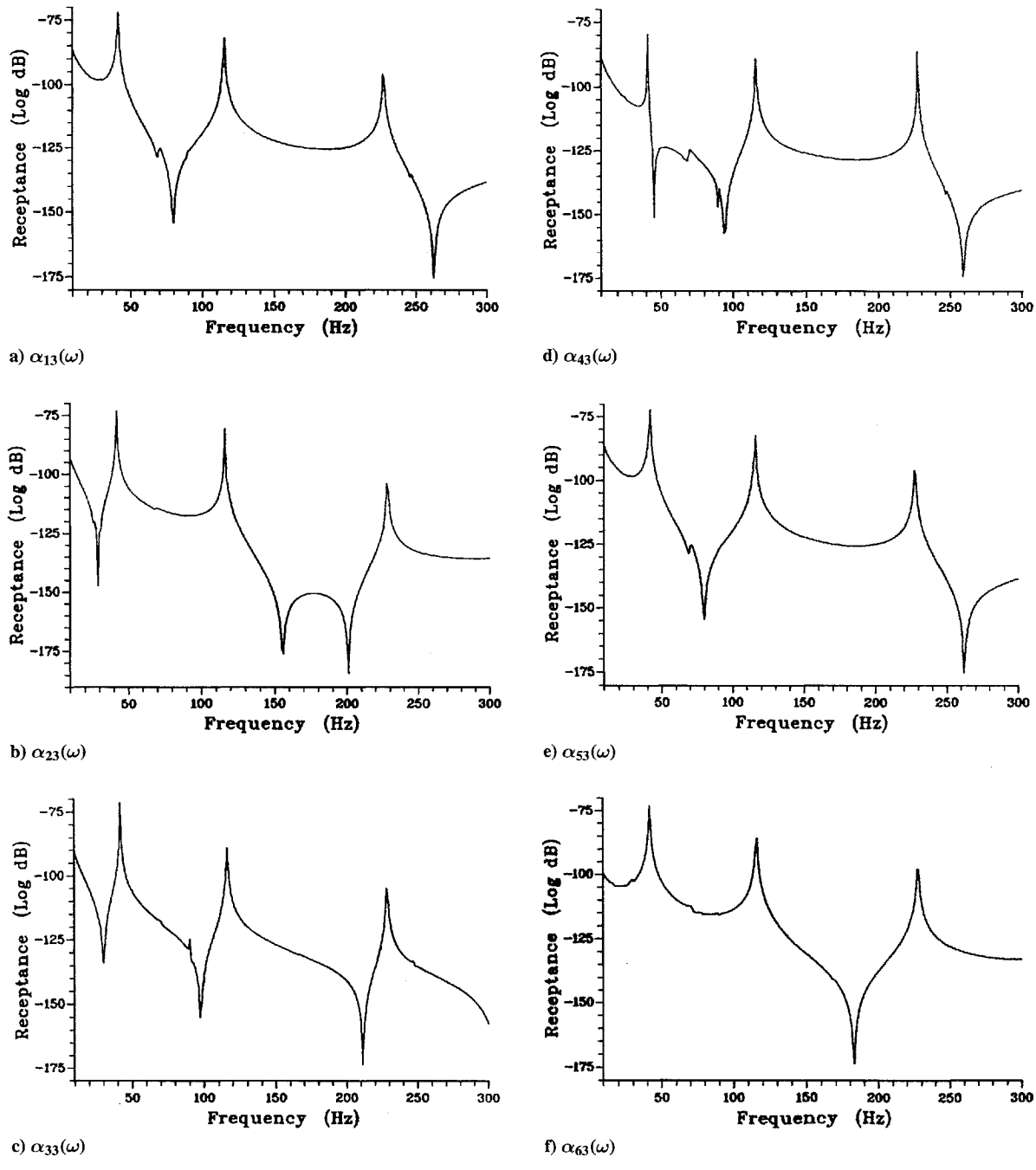

Fig. 7 Measured beam receptance data.

data is controlled by a computer using an in-house software specifically developed for step sine testing. Altogether six coordinates were measured along the beam as shown in Fig. 5 with excitation (shaker) being applied to coordinate x_3. These measured receptances are shown in Fig. 7 in a measurement frequency range of 10–300 Hz in which 350 frequency lines were measured and 3 bending modes were included. In the construction of $[A]$ and $[B]$ matrices, all of the six measured receptance FRFs were used with 330 data pairs ($L = 330$) and frequency separation of $\Delta n_k = q_k - p_k = 25$. With the thus constructed $[A]$ and $[B]$ matrices, natural frequencies, damping loss factors, and mode shapes for the three measured modes were identified. The identified natural frequencies are $\omega_1 = 41.81$ Hz, $\omega_2 = 116.10$ Hz, and $\omega_3 = 228.03$ Hz, and damping loss factors are $\eta_1 = 0.193\%$, $\eta_2 = 0.281\%$, and $\eta_3 = 0.205\%$. To check the identification accuracy, the identified modal parameters were then used to regenerate the receptance of $\alpha_{33}(\omega)$, which was then compared with its actual measured counterpart as shown in Fig. 8. As one can see, these two curves are very close, indicating that the identified modal parameters are quite accurate.

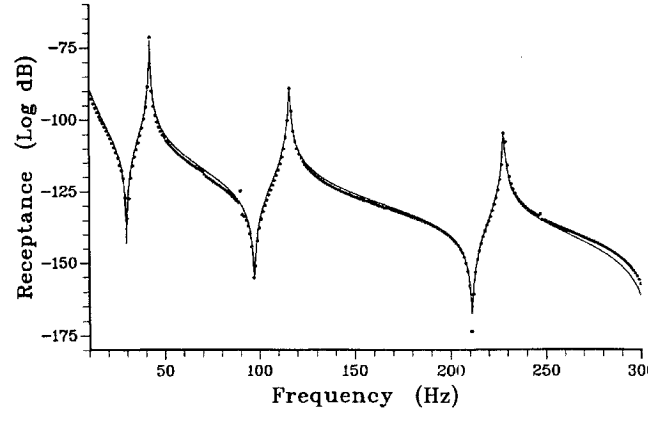

Fig. 8 Measured and regenerated receptances of beam test rig: * * *, simulated and ——, regenerated.

VI. Discussion and Conclusions

Eigenvalues and eigenvectors are the inherent properties of structural systems, and their identification should, in theory, be an eigenvalue problem. This is true when one computes eigenvalues and eigenvectors from known system mass, stiffness, and damping matrices. However, to identify them experimentally, there has been a missing link, which is the eigenvalue problem that links the required modal parameters and the measured FRF data. Most existing methods in frequency domain involve complicated curvefitting and interpolative procedures, thereby making the identification process unnecessarily complicated and the results identified often inaccurate and inconsistent.

The proposed method comes naturally to provide such a linkage. It calculates the modal parameters by solving an eigenvalue problem of an equivalent eigensystem derived from measured FRF data. All measured data are used simultaneously to construct the equivalent eigensystem matrices from which modal parameters of interest are solved. Because the identification problem is reduced to an eigenvalue problem of an equivalent system, natural frequencies and damping loss factors identified are consistent. Besides, the identified results are less sensitive to measurement errors than those from other existing methods since least squares procedure is used to estimate the derived system matrices and the eigensolution process involved is known to be numerically very stable. However, when measurement errors are present, spurious computational modes may arise in the frequency range of interest in addition to genuine physical modes that are of interest. These computational modes are generally easily identified since they vary considerably from one set of measured data to another.

Unlike other existing methods whose applications are often limited to analyzing FRFs of certain types of structure, the applicability of the proposed method is completely general. For linear structures, in addition to its application to ordinary structures that possess general levels of damping, it can also be applied to structures with very light damping whose analysis presents a problem for most SDOF based techniques and those with very high damping whose resonance phenomena are much less obvious and whose identifications pose a great difficulty to conventional modal analysis. For nonlinear structures, the method can be applied to extract accurate linear modal parameters required by analyzing off-resonance FRF data, and very accurate results have been obtained even when a strong nonlinear effect exhibits around resonances.

References

[1]Ewins, D. J., and Imregun, M., "State-of-the-Art Assessment of Structural Dynamic Response Analysis Methods (DYNAS)," *Shock and Vibration Bulletin*, Vol. 56, No. 1, 1986, pp. 59–90.

[2]Ewins, D. J., *Modal Testing: Theory and Practice*, Research Studies Press, London, 1984.

[3]Maia, N., "Extraction of Valid Modal Properties from Measured Data in Structural Vibration," Ph.D. Thesis, Mechanical Engineering Dept., Imperial College of Science, Technology, London, 1988.

[4]Brown, D., Allemang, R., Zimmeran, R., and Mergeay, M., "Parameter Estimation Technique for Modal Analysis," Society of Automotive Engineers, SAE TP 790221, 1979.

[5]Ibrahim, S., and Mikucik, E., "A Time-Domain Modal Vibration Test Technique," *Shock and Vibration Bulletin*, Vol. 43, No. 4, 1973, pp. 21–37.

[6]Ibrahim, S., and Mikucik, E., "The Experimental Determination of Vibration Parameters from Time Responses," *Shock and Vibration Bulletin*, Vol. 46, No. 3, 1976, pp. 187–196.

[7]Pappa, R. S., and Ibrahim, S. R., "A Parametric Study of the Ibrahim Time Domain Identification Algorithm," *Shock and Vibration Bulletin*, Vol. 51, No. 3, 1981, pp. 43–72.

[8]Pandit, S. M., and Wu, S. M., *Time Series and System Analysis with Applications*, Wiley, New York, 1983.

[9]Juang, J. N., and Pappa, R. S., "An Eigensystem Realization Algorithm (ERA) for Modal Parameter Identification and Model Reduction," *Journal of Guidance, Control, and Dynamics*, Vol. 8, No. 5, 1985, pp. 620–627.

[10]Juang, J. N., and Pappa, R. S., "Effect of Noise on Modal Parameters Identified by the Eigensystem Realization Algorithm," *Journal of Guidance, Control, and Dynamics*, Vol. 9, No. 3, 1986, pp. 294–303.

[11]Juang, J. N., "Mathematical Correlation of Modal-Parameter-Identification Methods Via System-Realization Theory," *International Journal of Analytical and Experimental Modal Analysis*, Vol. 2, No. 1, 1987, pp. 1–18.

[12]Pendered, J., and Bishop, R., "A Critical Introduction to Some Industrial Resonance Testing Techniques," *Journal of Mechanical Engineering Science*, Vol. 5, No. 4, 1963, pp. 368–378.

[13]Kennedy, C., and Puncu, C., "Use of Vectors in Vibration Measurement and Analysis," *Journal of the Aeronautical Sciences*, Vol. 14, No. 11, 1947.

[14]Dobson, B., "A Straight Line Technique for Extracting Modal Properties from Frequency Response Function Data," *Mechanical Systems and Signal Processing*, Vol. 1, No. 1, 1987, pp. 29–40.

[15]Ewins, D. J., and Gleeson, P., "A Method for Modal Identification of Lightly Damped Structures," *Journal of Sound and Vibration*, Vol. 84, No. 2, 1982, pp. 57–79.

[16]Vold, H., and Leuridan, J., "A Generalized Frequency Domain Matrix Estimation Method for Structural Parameter Identification," *Proceedings of the 7th Seminar on Modal Analysis* (Leuven, Belgium), 1982.

[17]Allemang, R. J., and Brown, D. L., "Multi-Input Experimental Modal Analysis—A Survey," *International Journal of Analytical and Experimental Modal Analysis*, Vol. 1, No. 1, 1986, pp. 37–44.

[18]Simon, M., and Tomlinson, G. R., "Use of Hilbert Transform in Modal Analysis of Linear and Nonlinear Structures," *Journal of Sound and Vibration*, Vol. 90, No. 2, 1984, pp. 275–282.

[19]Lin, R. M., Ewins, D. J., and Lim, M. K., "Identification of Nonlinearity from Analysis of Complex Modes," *International Journal of Analytical and Experimental Modal Analysis*, Vol. 8, No. 4, 1993, pp. 285–299.

[20]Lin, R. M., "Identification of Dynamic Characteristics of Nonlinear Structures," Ph.D. Thesis, Mechanical Engineering Dept., Imperial College of Science, Technology, London, 1991.

[21]Moler, C. B., and Steward, G. W., "An Algorithm for Generalized Matrix Eigenproblems," *SIAM Journal on Numerical Analysis*, Vol. 10, 1973, pp. 241–256.